Digital Optimal Robust Control

Meri Harutyunyan[1], Frédéric Holweck,[2,3] Dominique Sugny[1], and Stéphane Guérin[1,*]

[1]*Laboratoire Interdisciplinaire Carnot de Bourgogne, UMR CNRS 6303,*
Université de Bourgogne, BP 47870, F-21078 Dijon, France
[2]*Laboratoire Interdisciplinaire Carnot de Bourgogne, UMR CNRS 6303, UTBM, F-90010 Belfort, France*
[3]*Department of Mathematics and Statistics, Auburn University, Auburn, Alabama 36849, USA*

The lack of ability to determine and implement accurately quantum optimal control is a strong limitation to the development of quantum technologies. We propose a digital procedure based on a series of pulses where their amplitudes and (static) phases are designed from an optimal continuous-time protocol for given type and degree of robustness, determined from a geometric analysis. This digitalization combines the ease of implementation of composite pulses with the potential to achieve global optimality, i.e., to operate at the ultimate speed limit, even for a moderate number of control parameters. We demonstrate the protocol on IBM's quantum computers for a single qubit, obtaining a robust transfer with a series of Gaussian or square pulses in a time $T = 382$ ns for a moderate amplitude. We find that the digital solution is practically as fast as the continuous one for square subpulses with the same peak amplitudes.

Introduction.—Operating quantum technologies requires fast and accurate control of quantum systems [1,2]. Optimal control allows one to drive in principle the dynamics at the quantum speed limit [3]. In a two-level system, one can show that it coincides with a resonant square π pulse [4]. However, the final result depends on the quality of the pulse: for instance deviations of the amplitude (or of the time of interaction), referred to as pulse inhomogeneities, of order ε leads to an error of the same order for quantum gate. Improving robustness is thus vital to implement effective quantum information processing.

Adiabatic passage technique allows such robustness but at the cost of slow and inexact dynamics [5–7]. Composite pulse (CP) techniques, made of a π-pulse sequence with individual phases [8–14] or frequencies [15] as control parameters, are a powerful and simple tool for robust control. However, they are not optimal.

Optimal robust control aims at operating at the ultimate bounds (in time or energy) for given robustness criteria (pulse inhomogeneities, inhomogeneous broadening, etc.). The control pulses have thus the power to be resilient against fluctuations and uncertainties in the most optimal way with respect to a given cost (typically time of operation, area, or energy of the pulse). They have been derived using gradient-based algorithms (such as gradient ascent pulse engineering (GRAPE) [16,17]) or analytically from the Pontryagin's maximum principle [18,19]. Alternative methods based on inverse engineering geometric control have been also recently proposed [20,21]: the controls are determined from trajectories, devised from variational principles, in the dynamical parameter space. The latter, referred to as robust inverse optimization (RIO) [21–23], can be seen as an

optimal shortcut to adiabaticity technique [24–26]. It combines thus the robustness of composite pulses, formulated as constraint integrals for a given order, with time, area, or energy optimality. In the case of pulse inhomogeneities, the control features a constant amplitude and a time-continuous phase modulation.

Robustness to variations in system parameters is not the only key limitation to the experimental implementation of control protocols. Another hurdle relates to the ability of pulse-shaping devices to generate efficiently the theoretically designed driving process. With the notable exception of composite pulses, the majority of studies has assumed that the amplitude and phase of the control can vary continuously over time. This procedure is, however, problematic when the hardware is limited to a finite number of control parameters. Starting from the most general piecewise pulse shape and optimizing the corresponding free parameters present the difficulty of increasing the number of traps for a smaller number of parameters in the control landscape [27–29].

We propose in this Letter a digital optimal control to alleviate these limitations, where a digitalization, featuring a moderate number of parameters as amplitudes and static phases, has the power to mimic continuous controls and to explore the control landscape in a much simpler way. It is demonstrated in the case of qubit optimal robust control, for which the continuous analytic solution is known [22]. We consider specifically a digital version of RIO technique, referred to as DRIO, on IBM's quantum computers [30], based on superconducting transmon qubits [31].

Digital control has been originally proposed and explored in the context of adiabatic passage with a series

of femtosecond pulses [32] and in the context of stimulated Raman techniques [33–35]. A practical implementation of pulse trains driving a superconducting transmon has been investigated in [36]. This digitalization shares the ease of implementation of composite pulses (see, for instance, its recent implementation on IBM's computers [14]), but with the important difference that one uses subpulses of small area (much smaller than π) that allows a broader exploration of the control landscape in a way very close to the ideal optimal control functions.

Theory of digital control.—We consider a two-state system driven by a train of resonant subpulses, where each individual subpulse n, of duration τ, features the same shape $0 \leq \Lambda(t) \leq 1$, but has arbitrary phase φ_n and peak amplitude Ω_n. The digital Hamiltonian reads in the rotating wave approximation (in units such that $\hbar = 1$)

$$\hat{H}(t) = \frac{1}{2}\sum_n \Omega_n \mathbf{1}_n(t) \Lambda(t - t_n) \begin{bmatrix} 0 & e^{-i\varphi_n} \\ e^{i\varphi_n} & 0 \end{bmatrix}, \quad (1)$$

where the subpulse labeled n is centered at $t_n = n\tau$. We denote the indicator function on the interval I_n: $\mathbf{1}_n(t) = 1$ if $t \in I_n \equiv [t_{n-\frac{1}{2}}, t_{n+\frac{1}{2}}[$; 0 otherwise. The label n runs in principle from $-\infty$ to $+\infty$, i.e., $n = 0$ corresponds to the central pulse. We can consider Gaussian subpulses $\Lambda(t) = e^{-(t/\sigma)^2}$, that do not overlap, $\sigma \ll \tau$, typically of duration $\tau = 6\sigma$. Any other nonoverlapping pulse shape can be used since we show below that only the pulse area matters for the digitalization. In that situation, one can safely omit the indicator function from Hamiltonian (1) to which we associate the propagator $\hat{U}(t, t_i)$ (with t_i the initial time).

The peak Rabi frequency of the subpulse n can be sampled from a continuous pulse of shape $0 \leq \Pi(t) \leq 1$ and duration T

$$\Omega_n = \Omega_0 \Pi(t_n). \quad (2)$$

The phases φ_n form a piecewise constant function whose value varies from subpulse to subpulse that we want to sample from a continuous function: $\varphi_n = \varphi(t_n)$.

We show below that the digital model (1) can be made approximately equivalent to the effective continuous Hamiltonian (12). The general strategy is to derive the controls Ω_n, φ_n from the analysis of the continuous model (12), and to implement the digital control (1) efficiently with a number N of subpulses as low as possible.

Since the phase is constant for each subpulse, one can alternatively consider the Hamiltonian

$$\hat{H}_\delta(t) = \frac{1}{2}\sum_n A_n \delta(t - t_n) \begin{bmatrix} 0 & e^{-i\varphi_n} \\ e^{i\varphi_n} & 0 \end{bmatrix}, \quad (3)$$

associated to the propagator $\hat{U}_\delta(t, t_i)$, where the subpulse area $A_n = \Omega_n \int_{t_{n-\frac{1}{2}}}^{t_{n+\frac{1}{2}}} dt\, \Lambda(t - t_n) = \Omega_n \int dt \Lambda(t)$ between $t_{n\pm\frac{1}{2}} = (n \pm \frac{1}{2})\tau$ is concentrated into a Dirac δ pulse. One can indeed identify this propagator with the one of the original problem:

$$\hat{U}(t_{n+\frac{1}{2}}, t_{n-\frac{1}{2}}) = \hat{U}_\delta(t_{n+\frac{1}{2}}, t_{n-\frac{1}{2}}) = \hat{U}_\delta(t_n^+, t_n^-) \quad (4a)$$

$$= \begin{bmatrix} \cos(A_n/2) & -ie^{-i\varphi_n}\sin(A_n/2) \\ -ie^{i\varphi_n}\sin(A_n/2) & \cos(A_n/2) \end{bmatrix}, \quad (4b)$$

with $t_n^\pm$ denoting times immediately before and after $t_n = n\tau$, respectively. We highlight the fact that there is no additional phase coming from the time shifts $t_{n+\frac{1}{2}} \to t_n^+$ and $t_{n-\frac{1}{2}} \to t_n^-$ since the diagonal elements of the Hamiltonian are zero.

In the next step, we incorporate the phases in the wave function applying the piecewise constant transformation $T(t) = \text{diag}[e^{-i\sum_n \mathbf{1}_n(t)\varphi_n/2}, e^{i\sum_n \mathbf{1}_n(t)\varphi_n/2}]$:

$$H_\delta \equiv T^\dagger(t)\hat{H}_\delta T(t) - iT^\dagger(t)\frac{dT}{dt}$$

$$= \frac{1}{2}\sum_n \begin{bmatrix} -\delta(t - t_{n-\frac{1}{2}})\Delta\varphi_n & \delta(t - t_n)A_n \\ \delta(t - t_n)A_n & \delta(t - t_{n-\frac{1}{2}})\Delta\varphi_n \end{bmatrix} \quad (5)$$

with

$$\Delta\varphi_n = \varphi_n - \varphi_{n-1}. \quad (6)$$

The corresponding propagator $U_\delta(t, t_i)$ leads to the solution $\phi(t) = U_\delta(t, t_i)\phi(t_i) = T^\dagger(t)\Phi(t)$ with $\Phi(t)$ the state solution of the original problem (but with the Dirac δ pulses): $\Phi(t_n^+) = \hat{U}_\delta(t_n^+, t_n^-)\Phi(t_n^-)$, i.e.,

$$\Phi(t) = \hat{U}_\delta(t, t_i)\Phi(t_i) = T(t)U_\delta(t, t_i)T^\dagger(t_i)\Phi(t_i). \quad (7)$$

The Hamiltonian (5) is characterized by the superposition of two alternating trains of coupling and detuning terms, of total pulse area $\sum_n A_n$.

When $\Omega_n \equiv \Omega_0$ and $\varphi_n \equiv \varphi_0$ are constant for any n, i.e., $\Delta\varphi_n = 0$, the interaction is strictly periodic if one considers an infinite number of pulses and the Hamiltonian reads

$$H_\delta = \frac{A_0}{2\tau}\begin{bmatrix} 0 & 1 \\ 1 & 0 \end{bmatrix}\sum_k e^{ik\gamma t} \quad (8)$$

with the frequency of the pulse repetition $\gamma = 2\pi/\tau$. We have here used the Poisson formula for the Dirac distribution leading to the spectral representation of the Dirac comb, $\sum_n \delta(t - n\tau) = (1/\tau)\sum_k e^{ik\gamma t}$. When Ω_n and φ_n vary as functions of n, one can use the sampling property, $\sum_n f(n\tau)\delta(t - n\tau) = f(t)\sum_n \delta(t - n\tau)$, for a function $f(t)$, which leads to the Hamiltonian

$$H_\delta = \frac{1}{2\tau} \sum_k \begin{bmatrix} -e^{i\pi k}\Delta\varphi(t) & A(t) \\ A(t) & e^{i\pi k}\Delta\varphi(t) \end{bmatrix} e^{ik\gamma t} \quad (9)$$

such that $\Delta\varphi(t_{n-\frac{1}{2}}) = \Delta\varphi_n$, $A(t_n) = A_n$. If one considers piecewise constant Rabi frequencies of the form (2), one can define the function describing the instantaneous sub-pulse area

$$A(t) = \Omega_0 \Pi(t) \int ds\, \Lambda(s), \quad (10)$$

i.e., $A(t) = \sqrt{\pi}\sigma\Omega_0\Pi(t)$ for Gaussian subpulses or $A(t) = \Omega_0\tau\Pi(t)$ for square subpulses.

For the detuning, one can determine a continuous function from backward and forward Taylor expansions of the phase at time $t_{n-\frac{1}{2}}$: $\varphi_n = \varphi(t_n) = \varphi(t_{n-\frac{1}{2}}) + (\tau/2)\varphi'(t_{n-\frac{1}{2}}) + \cdots$, $\varphi_{n-1} = \varphi(t_{n-1}) = \varphi(t_{n-\frac{1}{2}}) - (\tau/2)\varphi'(t_{n-\frac{1}{2}}) + \cdots$, i.e.,

$$\Delta\varphi(t_{n-\frac{1}{2}}) = \tau\varphi'(t_{n-\frac{1}{2}}) + \frac{1}{3}\left(\frac{\tau}{2}\right)^3 \varphi'''(t_{n-\frac{1}{2}}) + \cdots$$
$$+ \frac{2}{(2p+1)!}\left(\frac{\tau}{2}\right)^{2p+1} \varphi^{(2p+1)}(t_{n-\frac{1}{2}}) + \cdots, \quad (11)$$

where $p \geq 0$ is an integer and extended at all times. At this stage, no approximation has been made in Hamiltonian (9) when one considers an infinite number of pulses, i.e., $T \gg \tau$.

The Hamiltonian (9) is not piecewise anymore, but it contains an infinite number of modes with the same amplitude $A(t)/2\tau$. The mode $k = 0$ is near resonant while the other ones can be considered as perturbation in the weak-field limit. At the lowest approximation, one only takes into account the resonant term $k = 0$, that we refer to as the second rotating wave approximation. This leads to the resonant effective Hamiltonian, including a correcting (second order) Stark shift (in units of 2τ) $S = \frac{1}{2}\sum_{k\neq 0}[A^2/(\Delta\varphi - 2\pi k)] \approx -(A^2/4\pi^2)\Delta\varphi \sum_{k\geq 1}(1/k^2) = -(A^2/24)\Delta\varphi$, which we identify with the continuous model according to

$$H_{\delta,0} = \frac{1}{2\tau}\begin{bmatrix} -(\Delta\varphi + S) & A \\ A & \Delta\varphi + S \end{bmatrix} \equiv \frac{1}{2}\begin{bmatrix} -\Delta & \Omega \\ \Omega & \Delta \end{bmatrix}. \quad (12)$$

The above effective Hamiltonian becomes a good approximation when $S \ll A$, i.e.,

$$A(t) \ll |2\pi - \Delta\varphi(t)|, \quad (13)$$

corresponding to a weak area of each subpulse, which is better satisfied for a larger number N of subpulses (for a given total pulse area). One can then identify an effective detuning $\Delta \equiv \Delta\varphi/\tau$ (omitting the Stark shift) and an effective Rabi frequency corresponding to the subpulse area divided by τ, $\Omega \equiv A(t)/\tau$. The effective (continuous) Hamiltonian (12) can be analyzed with standard techniques.

Digital robust inverse optimization.—We consider robust inverse optimization, where robustness is imposed with respect to pulse inhomogeneities (i.e., amplitude and/ or width) and optimization with respect to pulse duration, i.e., in minimum time (for a given pulse peak). At third order, the solution is a constant pulse of amplitude Ω, duration $T = 1.86\pi/\Omega$, and a detuning of Jacobi elliptic cosine form [21,22]

$$\Delta = \Delta_0 \text{cn}(\omega(t - t_i) + K(m), m), \quad t \in [t_i, t_i + T], \quad (14)$$

with $m = 0.235$, $\omega = 1.149\,\Omega$, and $\Delta_0 = 1.114\,\Omega$ for the problem of complete population transfer.

The peak amplitudes of the subpulses are constant $\Omega_n = \Omega_0$, since given by (2) where $\Pi(t) = 1$, with the Rabi coupling Ω_0 given by (10). We consider N subpulses, of area $A_n = A_0 = T\Omega/N$, giving the total duration $T = N\tau$. Assuming a phase variation of the order of π, one can reduce condition (13) to $T\Omega \ll \pi N$ for considering the sole $k = 0$ mode. This is in practice very well satisfied for N of the order of 10 as numerically determined. The phase $\varphi(t)$ is solution of (11), extended at all times: $\Delta = \varphi' + (\tau^2/24)\varphi''' + \cdots$. It is next digitalized at times t_n when the subpulses reach their peak value.

Figure 1 shows the dynamics of the continuous and digital RIO for $N = 15$ Gaussian or square subpulses. DRIO achieves a very good accuracy with an error in population transfer less than 10^{-4} when the approximation $\Delta = \varphi'$ is considered from (11). A time-optimal protocol of fifth-order robustness with respect to pulse inhomogeneities can be derived by following the techniques described in Ref. [21]. It gives a constant pulse of amplitude Ω and duration $T = 2.71\pi/\Omega$. The pulses and dynamics are shown in Fig. 2. Numerical studies show that, when we include the third-order derivative of (11), DRIO is much superior to a standard numerical time-discretization sampling by 1 order of magnitude for the same number N of samplings, allowing an approximation with an error less than 10^{-4} for a number of subpulses as low as $N = 9$.

Demonstration on IBM's quantum computer.—We performed the demonstration of the robustness profiles using IBM Quantum Experience [30]. It is built with superconducting transmon qubits, which can be controlled by microwave pulses. We used the low-level quantum computing QISKIT PULSE [37], as a module of the open-source framework QISKIT [38]. The processor used is *ibmq_manila*, which is one of the IBM five-qubit Falcon processors (Falcon r5.11L).

The parameters of the qubit, calibrated at the time of the experiment, are qubit transition frequency of 4.971 GHz, anharmonicity of -0.343 78 GHz, T_1 and T_2 coherence times of 153.89 μs and 46.19 μs, respectively, and readout error of 3%. We performed each experiment applying a sequence of Gaussian subpulses with the appropriate phase shifts, according to Figs. 1 and 2, respectively, where each
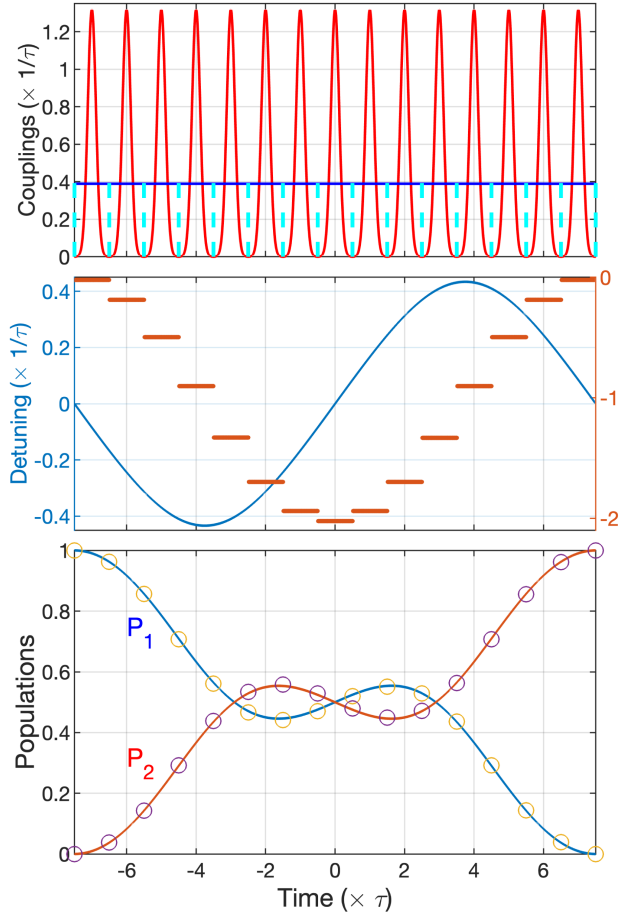
FIG. 1. Digital and continuous third-order RIO with $N = 15$ Gaussian-shaped or square subpulses. Upper frame: Rabi frequency pulse series $n = -7, \dots, 7$ with Gaussian-shaped (red line) or square subpulses (peak: horizontal blue line, delimited by dashed vertical lines) of individual duration τ and full duration $T = N\tau$; corresponding continuous constant Rabi frequency (horizontal blue line). Middle frame: detuning Δ and the corresponding digital (piecewise) phases $\varphi_n = \varphi(t_n)$ from $\Delta = \varphi'$. Lower frame: Population dynamics from the effective continuous model (12) (full line) and after each subpulse of the digital model (1) (circles), showing complete population transfers (exactly for continuous RIO, and with an error of less than 10^{-4} for DRIO). The total pulse area is 1.86π for both models.

single pulse has a duration of $\sigma = 3 \times \sqrt{2}$ ns. The total duration of the full process is $T = 382$ ns in both cases.

In Fig. 3, we have plotted the transition probability as a function of the deviation $-1 \leq \alpha \leq 1$ from the theoretical optimal value, $\Omega \to \Omega(1 + \alpha)$, with $\Omega = 1.86\pi/T$ (i.e., 15.3 MHz) and $\Omega = 2.71\pi/T$ (i.e., 22.3 MHz) for the third-order and fifth-order robustness, respectively. Each point corresponds to an experiment repeated 8096 times, where its value is averaged over the possible outputs 0 (ground) or 1 (excited state).

The experimental profiles of the single (square) Rabi pulse and of third- and fifth-order DRIO are compared with
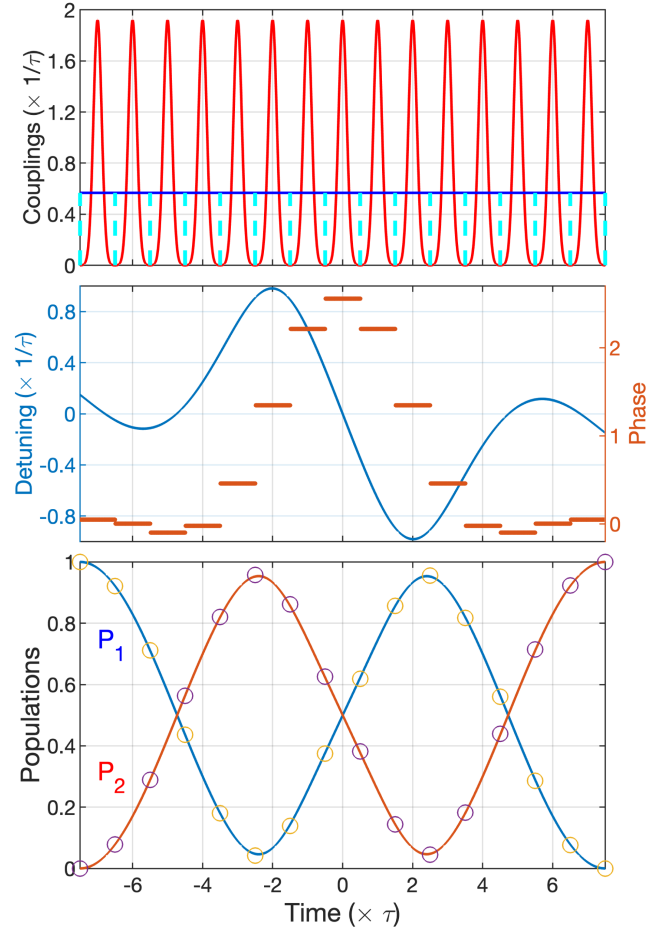
FIG. 2. Same as Fig. 1, but for the fifth-order RIO and DRIO, of total pulse area 2.71π.

the theoretical ones in Fig. 3. The small discrepancy, identical for DRIO and π-pulse excitations, amounts to approximately 3%, which corresponds to the systematic readout error. Apart this error, the experimental profiles fit remarkably well the theoretical predictions as shown by the profiles including 3% correction. We conclude that the DRIO protocol in principle features the same high-fidelity efficiency of the π-pulse method, but on a much broader interval.

Conclusions and discussion.—We demonstrated a digital optimal control procedure for realizing a robust one-qubit state-to-state transfer. It features a series of pulses, similarly to composite techniques, but where the control parameters are designed from a continuous-time control and has the potential to achieve global optimality. This approach has the decisive advantage of being able to account for the limitations of pulse-shaping devices using a moderate number of pulse parameters.

The demonstration is here provided for population transfer due to its simplicity (in particular from an experimental point of view). This can be directly applied for more complex processes such as quantum gate since, as we
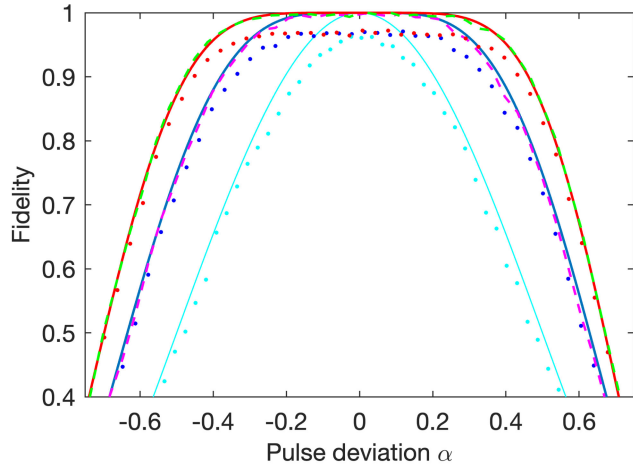
FIG. 3. Demonstration (dotted lines) of the digital π pulse (light blue), third- (dark blue) and fifth-order (red) DRIO robustness population profile (defining fidelity) as a function of the relative pulse amplitude deviation α, compared to their theoretical predictions (full lines). Experimental profiles corrected by the 3% measurement error (dashed magenta and green lines for third- and fifth-order, respectively) almost undistinguishable from the respective theoretical profiles.

have shown, the theoretical continuous form (provided in [22]) suffices to construct the digital procedure.

The applicability of the present digital robust control method on complex systems [39] depends on our ability (i) to generate the dynamical invariants allowing the construction of the state and propagator parametrization [40], from which one can implement the inverse engineering technique [see [41] for SU(2) symmetry] and (ii) to find the underlying Lagrangian multipliers (LMs) [21,23]. The dynamical invariants have been derived for SU(4) symmetry with interactions of the form $\sigma_i \otimes \sigma_i$, $\mathbb{1} \otimes \sigma_i$, $\sigma_i \otimes \mathbb{1}$, $i = x, y, z$ [42], which covers most of the practical applications of quantum computation involving two-qubit operations. One can reduce the dimensions using specific symmetries [43]. For instance, one can compensate the error in the phase of a two-qubit controlled-PHASE gate using SU(2)-symmetry interactions $T_1 \equiv \frac{1}{2}\sigma_x \otimes \sigma_x$, $T_2 \equiv \frac{1}{2}\sigma_x \otimes \sigma_y$, and $T_3 \equiv \frac{1}{2}\mathbb{1} \otimes \sigma_z$ [44]. An obstruction can arise when too many LMs are to be determined, typically more than 10. Robustness with respect to field inhomogeneities or inhomogeneous broadening requires (i) two LMs for population transfer and three LMs for single-qubit gate at third order; (ii) four LMs for complete (or partial) population transfer and six LMs for single-qubit gate (if we consider the trace fidelity) at fifth order. If one considers robustness against both amplitude and detuning, the number of LMs is doubled.

The performances of CPs are relatively close to the optimal ones for complete population transfer (third- and fifth-order robustness requiring 2π [22] and 3π [14] pulse areas, to be compared to the optimal 1.86π and 2.71π pulse

areas, respectively). However, RIO operates in a much faster way than CPs (with the same efficiency) for more complicated transfers or gates [22].

---

[*]Corresponding author: sguerin@u-bourgogne.fr

[1] M. A. Nielsen and I. L. Chuang, *Quantum Computation and Quantum Information* (Cambridge University Press, Cambridge, England, 2000).

[2] C. P. Koch, U. Boscain, T. Calarco, G. Dirr, S. Filipp, S. J. Glaser, R. Kosloff, S. Montangero, T. Schulte-Herbrüggen, D. Sugny, and F. K. Wilhelm, Quantum optimal control in quantum technologies. Strategic report on current status, visions and goals for research in Europe, Eur. Phys. J. Quantum Technol. **9**, 19 (2022).

[3] T. Caneva, M. Murphy, T. Calarco, R. Fazio, S. Montangero, V. Giovannetti, and G. E. Santoro, Optimal control at the quantum speed limit, Phys. Rev. Lett. **103**, 240501 (2009).

[4] U. Boscain, G. Charlot, J.-P. Gauthier, S. Guérin, and H. R. Jauslin, Optimal control in laser-induced population transfer for two- and three-level quantum systems, J. Math. Phys. (N.Y.) **43**, 2107 (2002).

[5] M. M. T. Loy, Observation of population inversion by optical adiabatic rapid passage, Phys. Rev. Lett. **32**, 814 (1974).

[6] L. P. Yatsenko, S. Guérin, and H. R. Jauslin, Topology of adiabatic passage, Phys. Rev. A **65**, 043407 (2002).

[7] N. V. Vitanov, A. A. Rangelov, B. W. Shore, and K. Bergmann, Stimulated Raman adiabatic passage in physics, chemistry, and beyond, Rev. Mod. Phys. **89**, 015006 (2017).

[8] S. Wimperis, Broadband, narrowband, and passband composite pulses for use in advanced NMR experiments, J. Magn. Reson. **109**, 221 (1994).

[9] H. K. Cummins, G. Llewellyn, and J. A. Jones, Tackling systematic errors in quantum logic gates with composite rotations, Phys. Rev. A **67**, 042308 (2003).

[10] B. T. Torosov, S. Guérin, and N. V. Vitanov, High-fidelity adiabatic passage by composite sequences of chirped pulses, Phys. Rev. Lett. **106**, 233001 (2011).

[11] J. A. Jones, Designing short robust NOT gates for quantum computation, Phys. Rev. A **87**, 052317 (2013).

[12] B. T. Torosov and N. V. Vitanov, Arbitrarily accurate variable rotations on the Bloch sphere by composite pulse sequences, Phys. Rev. A **99**, 013402 (2019).

[13] H. L. Gevorgyan and N. V. Vitanov, Ultrahigh-fidelity composite rotational quantum gates, Phys. Rev. A **104**, 012609 (2021).

[14] B. T. Torosov and N. V. Vitanov, Experimental demonstration of composite pulses on IBM's quantum computer, Phys. Rev. Appl. **18**, 034062 (2022).

[15] S. S. Ivanov, B. T. Torosov, and N. V. Vitanov, High-fidelity quantum control by polychromatic pulse trains, Phys. Rev. Lett. **129**, 240505 (2022).

[16] N. Khaneja, T. Reiss, C. Kehlet, T. Schulte-Herbrüggen, and S. J. Glaser, Design of NMR pulse sequences by gradient ascent algorithms, J. Magn. Reson. **172**, 296 (2005).

[17] K. Kozbar, S. Ehni, T. E. Skinner, S. J. Glaser, and B. Luy, Exploring the limits of broadband 90° and 180° universal rotation pulses, J. Magn. Reson. **225**, 142 (2012).

[18] L. Van Damme, Q. Ansel, S. J. Glaser, and D. Sugny, Robust optimal control of two-level quantum systems, Phys. Rev. A **95**, 063403 (2017).

[19] U. Boscain, M. Sigalotti, and D. Sugny, Introduction to the pontryagin maximum principle for quantum optimal control, PRX Quantum **2**, 030203 (2021).

[20] J. Zeng, C. H. Yang, A. S. Dzurak, and E. Barnes, Geometric formalism for constructing arbitrary single-qubit dynamically corrected gates, Phys. Rev. A **99**, 052321 (2019).

[21] G. Dridi, K. Liu, and S. Guérin, Optimal robust quantum control by inverse geometric optimization, Phys. Rev. Lett. **125**, 250403 (2020).

[22] X. Laforgue, G. Dridi, and S. Guérin, Optimal robust quantum control against pulse inhonomogeneities: Analytic solutions, Phys. Rev. A **106**, 052608 (2022).

[23] X. Laforgue, G. Dridi, and S. Guérin, Optimal robust stimulated Raman exact passage by inverse optimization, Phys. Rev. A **105**, 032807 (2022).

[24] A Ruschhaupt, X. Chen, D. Alonso, and J. G Muga, Optimally robust shortcuts to population inversion in two-level quantum systems, New J. Phys. **14**, 093040 (2012).

[25] D. Daems, A. Ruschhaupt, D. Sugny, and S. Guérin, Robust quantum control by a single-shot shaped pulse, Phys. Rev. Lett. **111**, 050404 (2013).

[26] D. Guéry-Odelin, A. Ruschhaupt, A. Kiely, E. Torrontegui, S. Martínez-Garaot, and J. G. Muga, Shortcuts to adiabaticity: Concepts, methods, and applications, Rev. Mod. Phys. **91**, 045001 (2019).

[27] T. E. Skinner and N. I. Gershenzon, Optimal control design of pulse shapes as analytic functions, J. Magn. Reson. **204**, 248 (2010).

[28] E. Dionis and D. Sugny, Time-optimal control of two-level quantum systems by piecewise constant pulses, Phys. Rev. A **107**, 032613 (2023).

[29] K. W. Moore and H. Rabitz, Exploring constrained quantum control landscapes, J. Chem. Phys. **137**, 134113 (2012).

[30] IBM Quantum, https://quantum-computing.ibm.com/.

[31] P. Krantz, M. Kjaergaard, F. Yan, T. P. Orlando, S. Gustavsson, and W. D. Oliver, A quantum engineer's guide to superconducting qubits, Appl. Phys. Rev. **6**, 021318 (2019).

[32] E. A. Shapiro, V. Milner, C. Menzel-Jones, and M. Shapiro, Piecewise adiabatic passage with a series of femtosecond pulses, Phys. Rev. Lett. **99**, 033002 (2007).

[33] J. A. Vaitkus and A. D. Greentree, Digital three-state adiabatic passage, Phys. Rev. A **87**, 063820 (2013).

[34] I. Paparelle, L. Moro, and E. Prati, Digital stimulated Raman passage by deep reinforcement learning, Phys. Lett. A **384**, 126266 (2020).

[35] J. A. Vaitkus, M. J. Steel, and A. D. Greentree, Digital waveguide adiabatic passage part 1: Theory, Opt. Express **25**, 5466 (2017); V. Ng, J. A. Vaitkus, Z. J. Chaboyer, T. Nguyen, J. M. Dawes, M. J. Withford, A. D. Greentree, and M. J. Steel, Digital waveguide adiabatic passage part 2: Experiment, Opt. Express **25**, 2552 (2017).

[36] E. Leonard Jr. *et al.*, Digital coherent control of a superconducting qubit, Phys. Rev. Appl. **11**, 014009 (2019).

[37] T. Alexander, N. Kanazawa, D. J. Egger, L. Capelluto, C. J. Wood, A. Javadi-Abhari, and D. McKay, QISKIT PULSE: Programming quantum computers through the cloud with pulses, Quantum Sci. Technol. **5**, 044006 (2020).

[38] G. Aleksandrowicz *et al.*, QISKIT: An Open-source Framework for Quantum Computing, 10.5281/zenodo.2562111 (2019).

[39] T. Schulte-Herbrüggen, A. Spörl, N. Khaneja, and S. J. Glaser, Optimal control-based efficient synthesis of building blocks of quantum algorithms: A perspective from network complexity towards time complexity, Phys. Rev. A **72**, 042331 (2005).

[40] H. R. Lewis and W. B. Riesenfeld, An exact quantum theory of the time-dependent harmonic oscillator and of a charged particle in a time-dependent electromagnetic field, J. Math. Phys. (N.Y.) **10**, 1458 (1969).

[41] X. Chen and J. G. Muga, Engineering of fast population transfer in three-level systems, Phys. Rev. A **86**, 033405 (2012).

[42] Utkan Güngördü, Y. Wan, M. A. Fasihi, and M. Nakahara, Dynamical invariants for quantum control of four-level systems, Phys. Rev. A **86**, 062312 (2012).

[43] F. T. Hioe, N-level quantum systems with SU(2) dynamic symmetry, J. Opt. Soc. Am. B **4**, 1327 (1987).

[44] S. S. Ivanov and N. V. Vitanov, Composite two-qubit gates, Phys. Rev. A **92**, 022333 (2015).